Matrix metalloproteinases are required for retinal ganglion cell axon guidance at select decision points

Carrie L. Hehr, Jennifer C. Hocking and Sarah McFarlane*

University of Calgary, 3330 Hospital Drive NW, Calgary, Alberta T2N 4N1, Canada
*Author for correspondence (e-mail: smcfarla@ucalgary.ca)

Summary

Axons receive guidance information from extrinsic cues in their environment in order to reach their targets. In the frog *Xenopus laevis*, retinal ganglion cell (RGC) axons make three key guidance decisions en route through the brain. First, they cross to the contralateral side of the brain at the optic chiasm. Second, they turn caudally in the mid-diencephalon. Finally, they must recognize the optic tectum as their target. The matrix metalloproteinase (MMP) and a disintegrin and metalloproteinase (ADAM) families are zinc (Zn)-dependent proteolytic enzymes. The latter functions in axon guidance, but a similar role has not yet been identified for the MMP family. Our previous work implicated metalloproteinases in the guidance decisions made by *Xenopus* RGC axons. To test specifically the importance of MMPs, we used two different in vivo exposed brain preparations in which RGC axons were exposed to an MMP-specific pharmacological inhibitor (SB-3CT), either as they reached the optic chiasm or as they extended through the diencephalon en route to the optic tectum. Interestingly, SB-3CT affected only two of the guidance decisions, with misrouting defects at the optic chiasm and tectum. Only at higher concentrations was RGC axon extension also impaired. These data implicate MMPs in the guidance of vertebrate axons, and suggest that different metalloproteinases function to regulate axon behaviour at distinct choice points: an MMP is important in guidance at the optic chiasm and the target, while either a different MMP or an ADAM is required for axons to make the turn in the mid-diencephalon.

Key words: *Xenopus laevis*, MMP2, MMP9, Growth cone, Target recognition, Optic chiasm

Introduction

The tip of the growing axon, the growth cone, reads cues in its environment in order to extend and reach its target. Receptors expressed by the growth cone bind to these cues and activate intracellular signalling, leading to changes in growth cone morphology and behaviour. A family of Zn-dependent proteolytic enzymes, the metalloproteinases, regulates cue-receptor interactions by cleavage of either guidance cues or their receptors (McFarlane et al., 2003). Two families of metalloproteinases, the matrix metalloproteinases (MMPs) and a disintegrin and metalloproteinases (ADAMs), are expressed in the developing nervous system (McFarlane, 2005; Yong et al., 2001). There are at least 20 MMPs in mammals, most of which are secreted molecules that function in remodelling of the extracellular matrix (ECM). The MMPs have been implicated in a number of pathological nervous system conditions (Yong et al., 2001). The ADAMs, a family of over 30 members, are generally transmembrane proteins. Various members of the ADAM and MMP families have been shown to regulate events such as the genesis, migration and survival of neurons in the developing embryo (McFarlane, 2005; Yong et al., 2001).

A role for metalloproteinases in axon extension and guidance is also emerging (McFarlane, 2003; McFarlane, 2005). Mutants of the *Drosophila* ADAM10 homologue *kuzbanian* exhibit both axon extension and guidance defects

(Fambrough et al., 1996; Schimmelpfeng et al., 2001). Two reports have indicated that, at least in culture, metalloproteinases are able to cleave axon guidance cues and receptors (Galko and Tessier-Lavigne, 2000; Hattori et al., 2000). The cleavage of ephrins and deleted in colorectal cancer (DCC), the receptor for the axon guidance molecule netrin, are inhibited by the application of broad-spectrum metalloproteinase inhibitors to embryonic neurons growing in culture. In both cases, metalloproteinases act to terminate axon guidance cue signalling. However, in other systems, cleavage that activates signalling has been reported (Diaz-Rodriguez et al., 1999; Mechtersheimer et al., 2001; Naus et al., 2004).

We recently showed in vivo that metalloproteinases are necessary for axon guidance in vertebrates (Webber et al., 2002). In the developing visual system of *Xenopus laevis*, retinal ganglion cell (RGC) axons make several guidance decisions en route to their major midbrain target, the optic tectum (Dingwell et al., 2000). We used an in vivo exposed brain preparation to demonstrate that metalloproteinases are necessary for at least two of the decisions (Webber et al., 2002). In the presence of a broad-spectrum hydroxamate-based metalloproteinase inhibitor, GM6001, RGC axons failed both to make a caudal turn in the mid-diencephalon and to recognize the optic tectum as their target.

As the hydroxamate-based inhibitors we used are known to block the activity of both ADAMs and MMPs, it is not clear

whether both metalloproteinase families are important for RGC axon guidance. To address this issue, we used a specific MMP pharmacological inhibitor in the *Xenopus* exposed brain preparation. MMP inhibitor IV (SB-3CT) selectively targets gelatinases by acting as a specific substrate that renders these metalloproteinases inactive (Brown et al., 2000; Kleifeld et al., 2001). The effects of blocking MMP function were distinct from those observed previously with GM6001 in that SB-3CT had no effect on the ability of RGC axons to make the turn in the mid-diencephalon, but caused defects in axon guidance at the optic tectum (Webber et al., 2002). Furthermore, we used a second in vivo preparation to show that both SB-3CT and GM6001 caused guidance defects at the optic chiasm. These results implicate MMPs, for the first time, in the process of axon guidance, and indicate that different metalloproteinases act at each axon choice point.

Materials and methods

Animals
Eggs were obtained from adult female *Xenopus laevis* stimulated with human chorionic gonadotrophin (Intervet Canada, Whitby, Ontario, Canada) and fertilized in vitro (Sive, 2000). Embryos were raised in 0.1× Marc's modified Ringer's solution (Sive, 2000) at 20-25°C and staged according to Nieuwkoop and Faber (Nieuwkoop and Faber, 1994).

Exposed brain and exposed optic chiasm preparations
The exposed brain preparation was performed as described previously (Chien et al., 1993; Webber et al., 2002). Briefly, embryos were anesthetized in modified Barth's solution (MBS) supplemented with 0.4 mg/ml tricaine (ethyl 3-aminobenzoate methane-sulfonic acid; Sigma, Oakville, Ontario, Canada), 50 mg/ml gentamicin sulfate (Sigma) and 10 mg/ml Phenol Red (Sigma). One set of experiments involved removing the skin and dura covering the left brain at stage 33/34 to expose the entire anterior brain on one side. In a second series of experiments, the optic chiasm was exposed at stage 30-31 by removing the cement gland and mesenchyme underlying the ventral forebrain. After surgery, the embryos were left to develop in either experimental or control MBS solutions for another 18-24 hours until they reached stage 40. The experimental solutions were MBS with 5-75 µM MMP2/MMP9 Inhibitor IV (SB-3CT; Chemicon, Temecula, CA), 100-400 µM of a specific peptide gelatinase inhibitor, cyclic CTTHWGFTLC (cyclic CTT) (Biomol, Plymouth Meeting, PA) or 5-10 µM GM6001 (Calbiochem, EMD Biosciences, Darmstadt, Germany). The control solution consisted of MBS (pH 7.4) with 0.05-0.4% dimethyl sulfoxide (DMSO), the solvent in which the inhibitor solutions were made. Compounds related to GM6001, N-t-butoxycaronyl-L-leucyl-L-tryptophan methylamide (Calbiochem, EMD Biosciences) and CTT, STTHWGFTLC (STT; Biomol) but with no effect on proteolytic activity were used as negative controls.

Visualization of the optic projection
The optic projection was visualized by anterogradely labelling RGC axons using horseradish peroxidase (HRP, type VI; Sigma) as described previously (Cornel and Holt, 1992). Briefly, the lens of the right eye was surgically removed and HRP dissolved in 1% lysolecithin was placed in the eye cavity. Embryos were fixed overnight in 4% paraformaldehyde in 0.1 M sodium phosphate buffer (pH 7.4). Dissected brains were washed in phosphate-buffered saline (PBS), reacted with diaminobenzidine (Sigma), dehydrated through a graded series of alcohols and cleared in 2:1 benzyl benzoate:benzyl alcohol. The outlines of brains and optic projections were drawn using a camera lucida attachment on a Zeiss (Thornwood, NY) microscope. All digital images in this study were taken with a Spot II camera and

Spot Advanced software (Diagnostics Instruments), and processed for brightness and contrast by using Adobe Photoshop (7.0) software. We used three reliable morphological landmarks to identify the anterior border of the tectum: the point where the second ventricle enlarges into the third, the posterior border of the neuropil of the tract of the posterior commissure and the position of the dorsolateral isthmus between the diencephalon and midbrain.

Quantification of optic projection length and turning angle
The effects of the MMP inhibitor were quantified by measuring the length and turning angle of optic projections in control and treated brains. Camera lucida representations were scanned with an Astra 1200s flatbed scanner (Umax, Freemont, CA) to provide digital images. Analysis was performed using the public domain NIH Image program. Brains were normalized by using macro programs described previously (Chien et al., 1993), by rotating and scaling them to a line drawn between the anterior optic chiasm and the midbrain-hindbrain isthmus. This line was matched to a standard reference line, artificially defined as 1 brain reference unit (b.r.u.); 1 b.r.u. is ~620 µm in an unfixed brain (Chien et al., 1993). The optic tract length was measured from the optic chiasm to the end of the optic projection, operationally defined as containing at least 10 axons. The angle through which the optic projection makes a turn in the mid-diencephalon was also measured (see Webber et al., 2002) (see Fig. 2A). A line (2) was drawn at a 60° angle to the reference line (1) between the optic chiasm and midbrain-hindbrain isthmus, bisecting the optic tract at the level of the turn made in the mid-diencephalon. The angle was measured between this line (2) and a line (3) drawn through the middle of the optic tract in its initial projection past the turn. Samples were compared statistically by using an unpaired ANOVA, followed by a Student-Newmann-Keuls multiple comparison post hoc test (Instat 2.0; GraphPad Software, San Diego, CA).

Immunocytochemistry
Embryos were exposed at stage 31 to either control media or media containing 25 µM SB-3CT. At stage 37/38, embryos were fixed overnight in 4% paraformaldehyde and 12 µm frozen transverse sections were cut through the brain and eyes by using a cryostat (Microm, San Marcos, CA). Briefly, sections were rinsed several times in PBT [PBS, 0.5% Triton (BDH), 0.1% bovine serum albumin (Sigma)], blocked in PBT+5% goat serum (Invitrogen Canada, Burlington, ON) and incubated overnight at 4°C in the primary antibody. Goat anti-mouse Rhodamine Red X (RRX) secondary antibodies (Jackson ImmunoResearch Laboratories, West Grove, PA; 1:500) were applied the next day for 1 hour at room temperature. After rinsing in PBT, samples were mounted in glycerol with an anti-bleaching agent, polyvinyl alcohol (Sigma). Primary antibodies were as follows: mouse 3CB2 [Developmental Studies Hybridoma Bank (DSHB), University of Iowa, IA; 1:10], mouse Zn-12 (DSHB; 1:40), mouse islet-1 (DSHB; 1:100) and rabbit GABA (Sigma, 1:3000).

In situ hybridization
Templates for riboprobe synthesis included a 1.5 kb fragment of the *Xenopus* MMP2 cDNA cloned into pBSK- (kindly provided by J.-C. Jung) (Jung et al., 2002), and the full coding region of *Xslit* (kindly provided by J. Wu) (Chen et al., 2000). Antisense digoxigenin-labelled riboprobe was transcribed with T7 RNA polymerase (Promega, Madison, WI). In situ hybridization was performed as described previously (Sive, 2000). Briefly, embryos were fixed in MEMFA (0.1 M MOPS, pH 7.4, 2 mM EGTA, 1 mM $MgSO_4$, 3.7% formaldehyde) for 1 hour and then dehydrated in ethanol and stored at –20°C until further use. Hybridization was performed overnight at 60°C. The probe was detected using alkaline phosphatase linked anti-digoxigenin antibodies and BM-Purple substrate (Roche, Mississauga, ON). Embryos were postfixed in Bouin's fixative (1% picric acid, 5% acetic acid, 9.25% formaldehyde), washed several times in buffered ethanol (70% ethanol, 30% PBS), rehydrated in PBS

and embedded in gelatin-albumin (Sigma) blocks for vibratome sectioning. Sections were cut at 50 μm on a Vibratome series 1000 (Ted Pella, Redding, CA), and then dehydrated through a series of alcohols. Finally, sections were cleared in xylene and mounted under glass coverslips with Permount (Fisher Scientific Company, Pittsburgh, PA).

Results

An MMP inhibitor causes defects in axon target recognition but not in the ability of axons to make a turn in the mid-diencephalon

Previously, we have found that two different broad-spectrum metalloproteinase inhibitors impaired RGC axon guidance decisions when applied to the developing optic projection in vivo (Webber et al., 2002). As these inhibitors are known to be effective against both MMPs and ADAMs, we asked in this study whether MMPs were important in the decisions made by extending RGC axons. As such, the specific MMP Inhibitor IV (SB-3CT) was applied to RGC axons extending in an in vivo exposed brain preparation (Brown et al., 2000; Chien et al., 1993; Webber et al., 2002). Brains were exposed at stage 33/34 when the first RGC axons have just entered the contralateral diencephalon. Embryos were then bathed either in a control solution containing DMSO, which was used to dilute the SB-3CT, or different concentrations (10-75 μM) of SB-3CT. These were slightly higher than those used previously in an in vitro study (Aye et al., 2004), but routinely higher concentrations of drug are required in the in vivo exposed brain preparation (McFarlane et al., 1995; Webber et al., 2002).

In control embryos, RGC axons extended dorsally, and then made a caudal turn in the mid-diencephalon before continuing on to their dorsal midbrain target, the optic tectum (Fig. 1A). In the presence of 10-25 μM of SB-3CT, the majority of RGC axons extended normally and made the diencephalic turn (Fig. 1B,C). However, upon reaching the optic tectum, many axons failed to recognize the tectum as their target and instead turned and grew dorsally. This phenotype was not observed in any of the control embryos ($n=36$), but increasing the SB-3CT concentration resulted in greater numbers of embryos with mistargeted axons; 22% ($n=18$) for 10 μM, 51% ($n=43$) for 25 μM, and 70% ($n=27$) for 50 μM. At higher concentrations (50-75 μM), the optic projections were often shorter than controls (Fig. 1D). Only one embryo had a shortened optic projection in control ($n=41$) and 10 μM SB-3CT-treated brains ($n=18$), whereas 23% ($n=47$) of 25 μM, 45% ($n=33$) of 50 μM and 60% ($n=15$) of 75 μM SB-3CT-treated brains exhibited RGC axon extension defects. Importantly, an unrelated cyclic peptide MMP (gelatinase) inhibitor, CTT (400 μM), produced a similar mistargeting phenotype (53%, $n=15$; compare Fig. 1B with 1F) (Koivunen et al., 1999). Similar concentrations were required to block migration of tumour and endothelial cells in vitro (Koivunen et al., 1999). By contrast, the optic projection formed normally when the brains were exposed to a closely related inactive peptide, STT (9/11) or to a control solution (8/8) (Fig. 1E). The fact, that two different inhibitors produce similar target recognition defects argues for the specificity of the effect for MMP inhibition.

To quantitate the effects of SB-3CT, two parameters were measured; the length of the optic projection and the angle
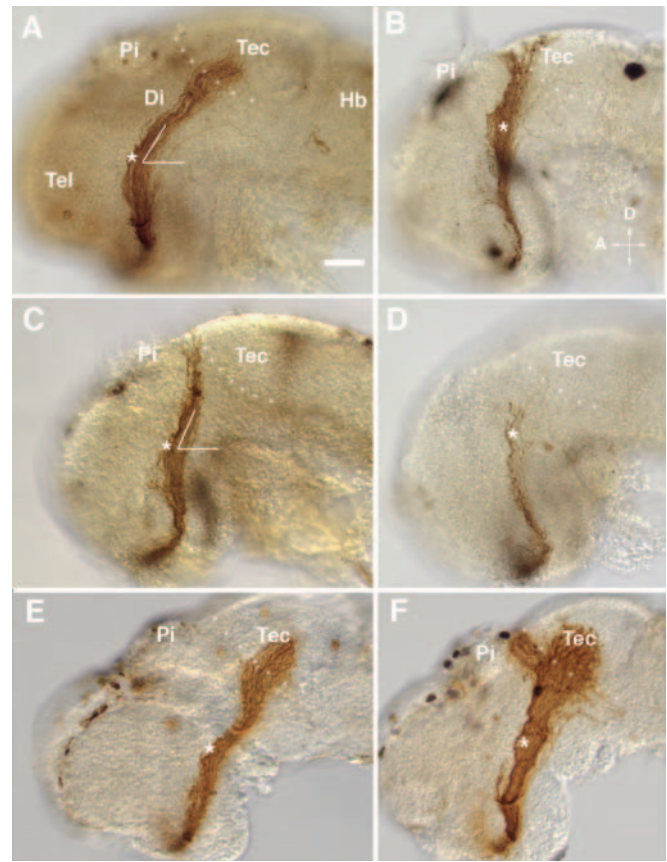
Fig. 1. The MMP inhibitor SB-3CT has differential effects on two guidance decisions made by RGC axons. Lateral views of the brains and HRP-labelled optic projections of stage 40 *Xenopus* embryos exposed at stage 33/34 to either control media or to the MMP-specific inhibitor IV (SB-3CT). (A) Control exposed brain. (B-D) Brains exposed to SB-3CT. At concentrations of 10 μM (B) and 25 μM (C) axons extend, make the turn in the mid-diencephalon (star), but are misguided at their target, the optic tectum. A demonstration of the turning angle at the mid-diencephalon is shown in A and C. By contrast, in GM6001-treated brains we found that axons failed to make the turn, and instead grew towards the pineal gland (Webber et al., 2002). (D) With a higher concentration (50 μM) of the inhibitor, axon extension defects are sometime seen. (E,F) A cyclic peptide MMP inhibitor, CTT, produces a similar mistargeting phenotype (F), while a highly related inactive peptide, STT, has no effect on the optic projection (E). The white dots indicate the approximate anterior of the optic tectum (see Materials and methods). D, dorsal; A, anterior; Tec, tectum; Tel, telencephalon; Di, diencephalon; Pi, pineal gland; Hb, hindbrain. Scale bar: 50 μm.

through which RGC axons make a turn in the mid-diencephalon. Previously, we have found that GM6001 altered the turning angle of RGC axons at the mid-diencephalic turn, implicating metalloproteinases in this guidance decision (Webber et al., 2002). In GM6001-treated brains, axons failed to make the turn, and, as such, grew towards the pineal gland and never reached the anterior border of the optic tectum. By contrast, axons in SB-3CT-treated brains made the turn in the mid-diencephalon, ultimately reached the tectal border, and then failed to recognize their target. In agreement, similar turning angles were observed for control and SB-3CT treated

embryos (Fig. 2A), which argues that an SB-3CT sensitive MMP is not important at the mid-diencephalic guidance choice point. Interestingly, the optic projection length was relatively unaffected by the low inhibitor doses (10 and 25 μM) that caused guidance defects, but was inhibited significantly at higher concentrations (Fig. 2B).
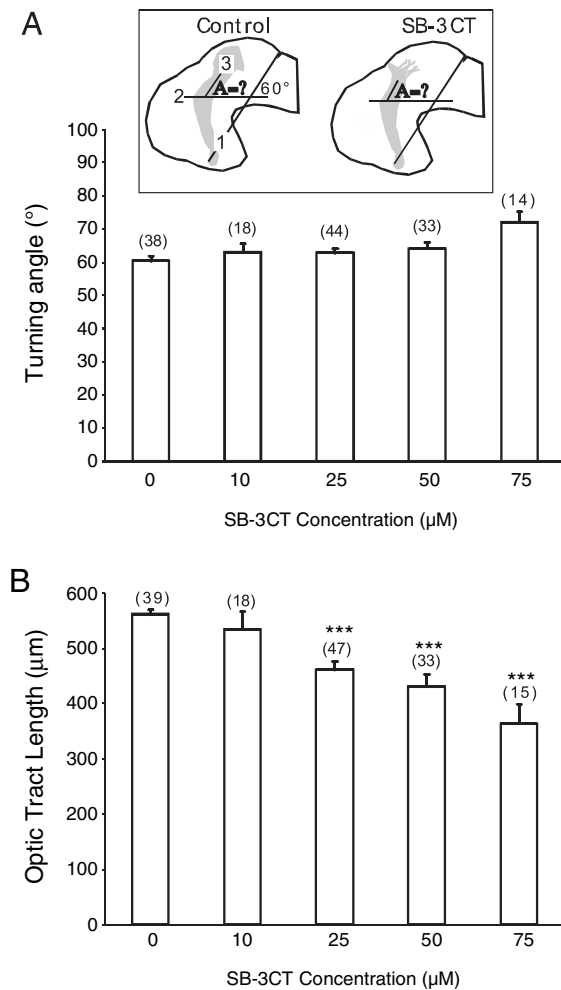

Fig. 2. Quantitation of the effects of SB-3CT on RGC axon outgrowth. Camera lucida representations of the brains and optic projections of control and treated embryos were digitized and analyzed for two measures of optic projection development: the mean angle through which RGC axons turned at the mid-diencephalon (A); and the length of the optic projection (B). (A) Dose-response curve for SB-3CT effects on the mean turning angle. The inset shows a schematic of how the turning angle was measured for a control and a SB-3CT-treated brain. Briefly, a standard reference line (1) was drawn between the optic chiasm and the midbrain-hindbrain boundary. A second line (2) was drawn at a 60° angle to line 1, and the angle through which the RGC axons turn in the mid-diencephalon was measured as the angle between line 2 and a third line (3) drawn through the middle of the optic projection just after the turn. A demonstration of the turning angle at the mid-diencephalon is shown in Fig. 1A,C. (B) Dose-response curve for SB-3CT effects on the optic projection length. Error bars are s.e.m., and numbers in brackets represent the number of optic projections analyzed. (***$P<0.001$; one-way ANOVA, Student-Newmann Keuls post-hoc comparisons test).

The MMP inhibitor causes severe extension defects as well as guidance errors at the optic chiasm

The data outlined above argue that a metalloproteinase(s), but not an SB-3CT-sensitive MMP, is involved in the decision to make a turn in the mid-diencephalon. To examine whether MMPs and/or ADAMs function in the guidance of RGC axons at other decision points, we developed a new in vivo preparation to examine guidance at the optic chiasm. The exposed optic chiasm preparation is similar in principle to that of the exposed brain preparation. However, exposures were made several hours earlier, between stages 30-31, just prior to when the first RGC axons reach the optic chiasm (Holt, 1989). The skin and mesenchyme overlying the most ventral region of the forebrain were removed. These embryos were grown in a control bath, or in media containing either the MMP inhibitor or the broad spectrum metalloproteinase inhibitor, GM6001. Thus, we could determine the relative importance of the different metalloproteinase families in guidance at the optic chiasm. At stage 40, RGC axons were visualized by anterograde HRP labelling.

The two metalloproteinase inhibitors had similar effects on axon behaviour in the ventral forebrain (Fig. 3). In control embryos (62/70), or embryos exposed to a chemical related to GM6001 but unable to inactivate metalloproteinases (GM6001 negative control) (55/62), axons extended normally into the contralateral diencephalon (Fig. 3A,B). By contrast, few embryos had normal optic projections upon treatment with the metalloproteinase inhibitors. With 25 μM SB-3CT, only 2/22 embryos had optic projections that reached the dorsal
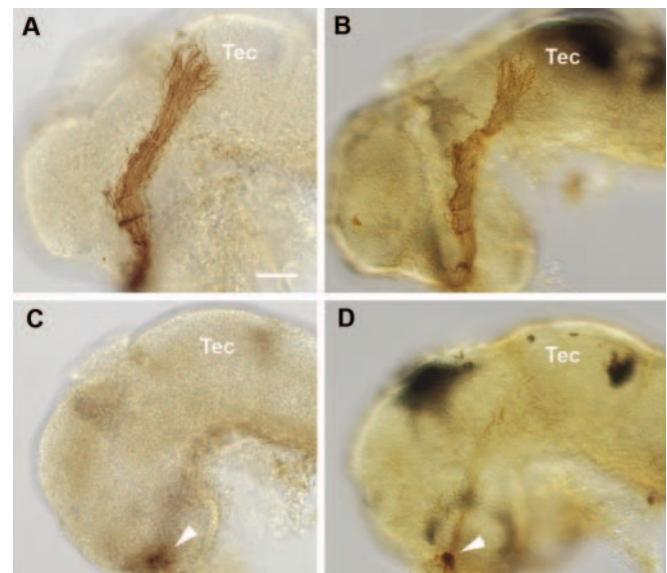
Fig. 3. RGC axons that cross the optic chiasm in the presence of metalloproteinase inhibitors fail to extend into the contralateral diencephalon. The optic chiasm was exposed at stage 30-31, by removing the cement gland and the mesenchyme underlying the ventral forebrain. Embryos were bathed in control media (A) or in media to which either the broad-spectrum metalloproteinase inhibitor GM6001 (5-10 μM; D), SB-3CT (25 μM; C) or the GM6001 negative control (5-10 μM; B) was added. At stage 40, RGC axons were anterogradely labelled with HRP. In GM6001 and SB-3CT, the optic projection (arrowhead) failed to enter the contralateral diencephalon. Tec, tectum. Scale bar: 50 μm.

diencephalon. The remaining SB-3CT-treated embryos had shorter optic projections, and the vast majority of these projections failed to enter the contralateral diencephalon
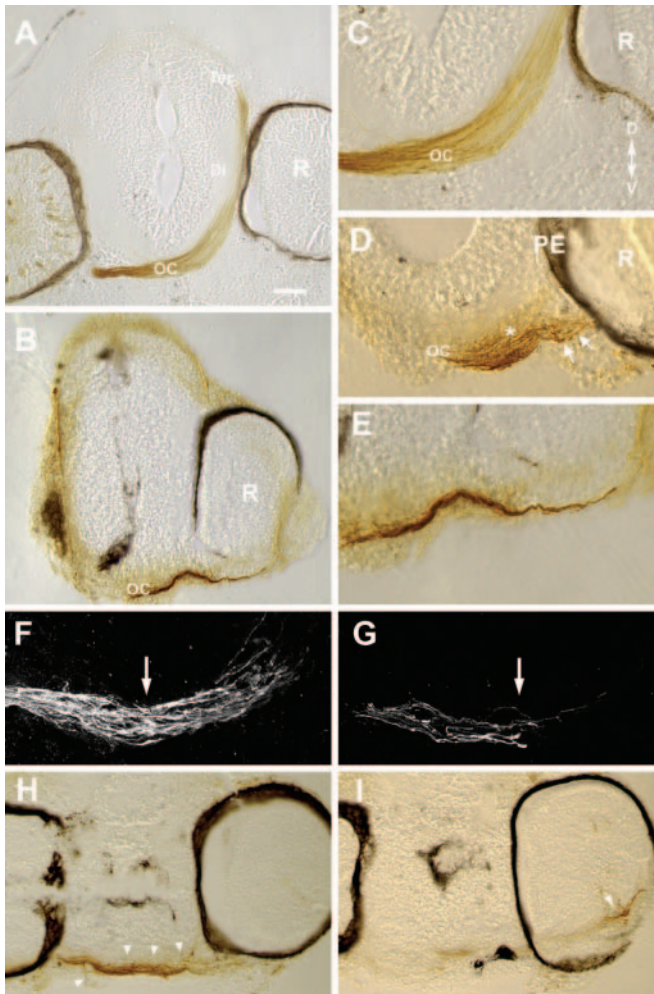
Fig. 4. Axon guidance defects caused by application of metalloproteinase inhibitors as RGC axons cross the optic chiasm. Vibratome (50 μm) sections through the diencephalon and eyes of embryos exposed at stage 31 to either control (A,C), SB-3CT (B,D,E) or GM6001 (H,I) solutions. The HRP-labelled optic projections are visible. (A,C) In control, RGC axons cross the midline at the optic chiasm and grow dorsally through the diencephalon to innervate the optic tectum. C is a higher power view of the optic chiasm shown in A. (B,D,E) In the 25 μM SB-3CT-treated brains, RGC axons often failed to enter the contralateral diencephalon (star), or grew aberrantly into the contralateral optic nerve (arrows). E is a higher power view of the optic projection shown in B and D is another example of a 25 μM SB-3CT-treated brain. (F,G) Fluorescent micrographs of the HRP-labelled optic projections in 12 μm transverse cryostat sections through the optic chiasm in the ventral diencephalon. Control axons shown in F cross the midline (arrow), whereas SB-3CT treated axons (G) stalled at the midline (arrow). (G) A more weakly labelled optic projection was chosen for visualization purposes. (H,I) Similar axonal phenotypes are observed in a 10 μM GM6001-treated brain. (H) Axons in the optic chiasm are seen to defasciculate (arrowheads). In a more caudal section (I), axons are seen within the contralateral eye (arrowhead). Tec, tectum; D, dorsal; V, ventral; oc, optic chiasm; R, retina. Scale bar: 50 μm for A,B,H,I; 25 μm for C-G.

altogether (14/20) (Fig. 3C). Interestingly, these severe axon extension defects were observed at a concentration of SB-3CT that had little effect on axon extension in the exposed brain preparation (see Fig. 1B, Fig. 2B). Similar defects in axon extension were observed with GM6001. With both 5 and 10 μM GM6001, the predominant defect was for axons to fail to project into the contralateral diencephalon (9/33 of embryos with 5 μM GM6001 and 28/35 of embryos with 10 μM GM6001) (Fig. 3D). Significantly, 5 μM GM6001 had no effect on its own on basal RGC neurite extension in vitro (data not shown), which argues that in vivo the metalloproteinase inhibitors are affecting axon outgrowth regulated by extrinsic cues.

To examine the behaviour of RGC axons at the optic chiasm, HRP-labelled RGC axons were followed in 50 μm vibratome sections through the eyes and diencephalon of stage 40 embryos. It was clear that in the control brains for SB-3CT, the majority of RGC axons crossed at the optic chiasm (5/6 embryos) and extended into the ventral diencephalon and dorsally towards the optic tectum (Fig. 4A,C). In contrast, in the majority of 25 μM SB-3CT treated brains (10/13), axons failed to enter the contralateral ventral diencephalon (Fig. 4B,D,E). In these brains, axons appeared to either stall at the optic chiasm (Fig. 4G), or were misrouted and grew into the contralateral optic nerve (Fig. 4D,E). Similar defects were seen in GM6001-treated embryos (16/23) (Fig. 4H,I), but not in their corresponding controls (control, 2/23; GM6001 negative control, 2/27). In addition, GM6001 sometimes caused defasciculation of the optic projection at the optic chiasm (8/23 embryos), a phenotype not observed with SB-3CT (1/13 embryos) (compare Fig. 4A with 4H). These data argue that metalloproteinases, and probably an MMP, are required for axon guidance and extension at the optic chiasm.

SB-3CT causes no obvious defects in the optic pathway from the retina to the ventral diencephalon

SB-3CT could cause defects in the behaviour of RGC axons in the ventral diencephalon via non-specific disruption of the optic pathway. To ensure that the retinas, optic nerve and ventral diencephalon developed normally in SB-3CT-treated brains we examined the expression of a number of markers in embryos treated in the exposed chiasm preparation with either a control solution or 25 μM SB-3CT. We found that:

(1) mRNA expression of the guidance molecule *Xslit* (Chen et al., 2000) was similar to control within the ventral diencephalon at the optic chiasm (Fig. 5A,B). Moreover, expression of *Xslit* within the anterior lobe of the pituitary body, just ventral to the optic chiasm, was maintained in SB-3CT-treated embryos.

(2) Layering within the treated retinas was normal, as assessed by expression of the neurotransmitter γ-amino butyric acid (GABA) (Fig. 5K,L) and *Xslit* mRNA (Fig. 5C,D) by amacrine cells of the inner nuclear layer; by expression of the transcription factor islet 1 within the RGC and inner nuclear layers (Fig. 5I,J); and by expression of the glial cell antigen 3CB2 (Fig. 5E,F) (Prada et al., 1995).

(3) Glial cell expression of the 3CB2 antigen was maintained in the optic nerve (Fig. 5G,H).

(4) The ventral nature of the diencephalon was maintained by immunolabelling with antibodies against 3CB2 (Fig. 5E,H),
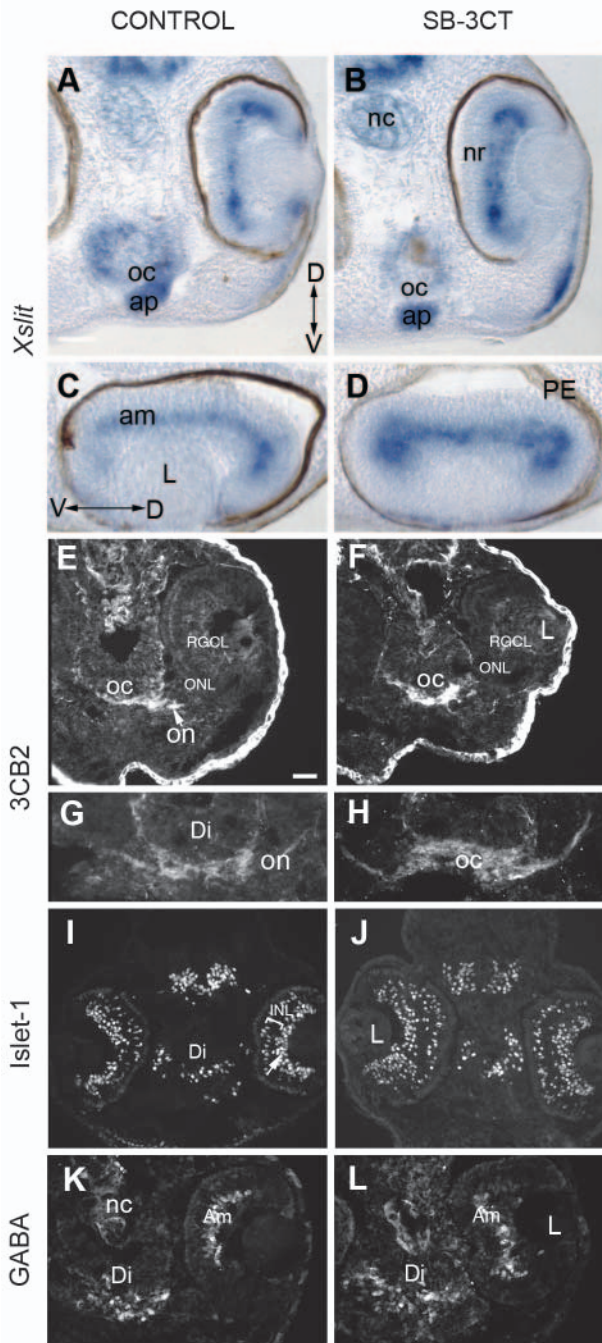
Fig. 5. Optic pathway apparently unaffected by MMP inhibition. Embryos were exposed at stage 31 to either a control solution (A,C,E,G,I,K) or 25 μM SB-3CT (B,D,F,H,J,L). At stage 37/38, embryos were fixed. (A-D) Embryos were processed as wholemounts for in situ hybridization for *Xenopus slit* mRNA. Vibratome sections (50 μm) were cut. The ventral diencephalon at the level of the optic chiasm is represented in A,B, and eye sections are shown in C,D. (E-H) Immunoreactivity for the glial cell marker 3CB2. (G,H) Higher power views of E,F, showing the optic nerves and the optic chiasm in the ventral diencephalon. (I,J) Islet 1 immunoreactivity showing label in the ventral region of the diencephalon adjacent to the optic chiasm, and labelling of RGCs and cells in the inner nuclear layer in the retina. (K,L) GABA immunoreactivity showing labelling of amacrine cells in the inner nuclear layer, and a population of neurons in the ventral diencephalon. L, lens; nc, notochord; ap, anterior lobe of the pituitary body; nr, neural retina; PE, pigment epithelium; oc, optic chiasm; on, optic nerve, RGCL, RGC layer; Am, amacrine cells; INL, inner nuclear layer; ONL, outer nuclear layer; Di, diencephalon. D, dorsal; V, ventral. Orientation in A is for A,B,E,L, and orientation in C is for C,D. Scale bars: in A, 50 μm for A,B; 25 μm for C,D; in E, 50 μm for E,F,I,L; 25 μm for G,H.

and axons, and can be secreted by the growth cone (Agapova et al., 2001; Zuo et al., 1998). Thus, we examined the spatiotemporal pattern of expression of *Xenopus mmp2* (*Xmmp2*) mRNA, which to date has only been examined at *Xenopus* metamorphosis (Jung et al., 2002). Embryos at different developmental stages were processed for in situ hybridization with a digoxigenin-labelled antisense RNA probe for *Xmmp2*. At stage 32, when RGC axons are crossing the optic chiasm, *Xmmp2* is expressed in the mesenchyme underlying the optic chiasm, but apparently is not expressed in the brain or by RGCs (Fig. 6A). Importantly, like most MMPs, XMMP2 is a secreted protein and can presumably act at a distance from the cells that make it (Jung et al., 2002). At stage 35/36, the first RGC axons have reached the mid-diencephalon and make a caudally directed turn. *Xmmp2* is not expressed near the in growing RGC axons in the mid-diencephalon at this stage, but is expressed in tissue overlying the optic tectum (Fig. 6B). The mRNA continues to be expressed in this region at stage 37/38, when the first RGC axons are reaching the optic tectum. These data, together with the guidance defects observed with SB-3CT and CTT, indicate that MMP2 could act within the ECM to regulate signalling between guidance cues and their receptors in order to influence the behaviour of RGC axons.

Discussion

To the best of our knowledge, this paper demonstrates for the first time that MMPs are involved in axon guidance. Although ADAM proteins have been implicated in axon guidance in species from worms to mice (Fambrough et al., 1996; Hattori et al., 2000; Huang et al., 2003; Nishiwaki et al., 2000), this has not been true of MMPs. We show that when a drug specifically engineered to inhibit MMP gelatinases was applied to the developing optic projection, two out of three key guidance decisions made by RGC axons travelling in the brain were affected. First, axons failed to enter the contralateral brain and instead either stalled at the optic chiasm, or grew aberrantly towards the contralateral eye. Second, axons exposed to the inhibitor after crossing into the contralateral brain correctly made a crucial turn in the mid-diencephalon,

islet 1 (Fig. 5I,J) and GABA (Fig. 5K,L). These data argue that the defects caused by the metalloproteinase inhibitors are not due to gross disruption of the optic pathway.

MMP2 is expressed alongside the optic tract

In vitro analysis has shown that SB-3CT has a 1000-fold greater specificity for MMP2 and MMP9 over other MMPs examined (Brown et al., 2000). Similarly, CTT is thought to be more specific for the MMP2/MMP9 gelatinases (Koivunen et al., 1999). However, although embryonic mouse RGCs express MMP9, this does not appear to be the case in *Xenopus* (Carinato et al., 2000). MMP2 seemed a likely candidate to influence RGC axon outgrowth, as it is expressed by adult human RGCs

Fig. 6. MMP2 is expressed in tissues that abut the developing visual system. Embryos at stages 32 (A) and 35/36 (B) were processed as wholemounts for in situ hybridization with a digoxigenin-labelled (blue) *XMMP2* antisense riboprobe. Vibratome transverse sections (50 μm) through the embryo at the level of the diencephalon. Pigmented cells are shown in black. Broken line represents the ventral diencephalon, with the optic chiasm found at the midline. The arrowheads point to *Xmmp2* mRNA-expressing cells that neighbour the optic tectum. R, retina; oc, optic chiasm; Tec, tectum; Ve, ventricle; D, dorsal, V, ventral. Scale bar: 50 μm.

but subsequently avoided the optic tectum. Thus, an MMP(s), possibly MMP2, functions at the optic chiasm and tectum to ensure the accuracy of RGC axon pathfinding.

There is growing support for the idea that metalloproteinases are crucial regulators of axon extension and guidance (McFarlane, 2003). The bulk of the evidence rests on the use of broad-spectrum metalloproteinase inhibitors, which fail to discriminate between MMP and ADAM family members. Investigations of individual metalloproteinases have revealed functions for ADAMs in axon extension and guidance (Fambrough et al., 1996; Hattori et al., 2000; Huang et al., 2003; Leighton et al., 2001; Schimmelpfeng et al., 2001). By contrast, no central nervous system defects were reported for flies mutant for both of the two *Drosophila* MMPs (Page-McCaw et al., 2003). And axon guidance defects have not been reported in the various mice deficient for individual MMPs (reviewed by Johnson et al., 1998; McFarlane, 2005). This may reflect that more subtle defects were overlooked, that compensation occurred through upregulation of other MMPs or that there is considerable redundancy in this large family of metalloproteinases.

Certainly, a number of MMPs, including MMP2, are expressed in the growth cones of vertebrate neurites extending in vitro (Chambaut-Guerin et al., 2000; Hayashita-Kinoh et al., 2001; Nordstrom et al., 1995; Zuo et al., 1998). There is a suggestion from the literature that MMPs act to degrade the ECM to ease the movement of an axon forwards, as growth factor-treated pheochromocytoma cells that express antisense mRNA for stromelysin-1/MMP3 have problems extending through a basal lamina culture matrix (Nordstrom et al., 1995). Our data indicate that the role of MMPs in axon guidance is not simply to digest a path through the ECM via which RGC axons can extend, in that axon guidance defects were observed

at SB-3CT doses with little or no effect on axon extension. Thus, it is likely that MMPs directly cleave RGC axon guidance cues or the growth cone receptors, as is the case for ADAMs (Galko and Tessier-Lavigne, 2000; Hattori et al., 2000). A comparison of our SB-3CT and GM6001 data supports the idea that both ADAMs and MMPs are required for the proper guidance of RGC axons. For example, at the optic chiasm GM6001 and the MMP inhibitor showed overlapping, but distinct axon guidance phenotypes: defasciculation was observed only with GM6001 treatment.

It is unclear whether metalloproteinases function directly in RGC growth cones, or in the substrate through which they extend. The growth cones of a number of different neurons express MMPs (Chambaut-Guerin et al., 2000; Hayashita-Kinoh et al., 2001; Nordstrom et al., 1995; Zuo et al., 1998). However, MMP2 is expressed by tissues surrounding the optic pathway, and not by RGCs. Thus, MMP2 may be secreted and diffuse into the optic pathway to influence the behaviour of RGC axons. The fact that two chemically distinct MMP2/MMP9-specific inhibitors produced similar mistargeting phenotypes lends support for such a role for MMP2. A caveat is that in the exposed brain and chiasm experiments, a significant amount of MMP2-expressing tissue would have been removed surgically. It is likely that enough MMP2 expressing tissue remained in both experimental preparations or that MMP2 was secreted and diffused to the optic pathway prior to surgery, and thus was present in the exposed preparations. The possibility remains, however, that another MMP(s) is inhibited by SB-3CT and is the one that is important in RGC axon guidance. For example, MMP11 and MMP13 are expressed in the *Xenopus* eye at stages when RGC axons extend through the brain (Damjanovski et al., 2000). The inhibitor was designed to specifically target gelatinases, and inhibits MMP2 and MMP9 at 1000-fold lower concentrations than other MMPs (Brown et al., 2000). Although, in general, higher concentrations are required in vivo than in vitro, it is possible that the SB-3CT concentrations used in our experiments blocked other MMPs not officially classified as gelatinases, but that can cleave this substrate (Brown et al., 2000; Isaksen and Fagerhol, 2001).

Our data argue that an MMP(s) functions in some but not all guidance decisions within the diencephalon. However, the GM6001 results indicate that metalloproteinase function is required at all the decision points we have examined (Webber et al., 2003). Thus, guidance in the mid-diencephalon and fasciculation of axons at the optic chiasm, which were specifically affected by GM6001, probably requires either an ADAM or a non-gelatin processing MMP. Thus, different metalloproteinases may function in the guidance of RGC axons in distinct brain regions. A second possibility is that the guidance cues targeted by MMPs vary along the optic pathway. Certainly, guidance cues show distinct expression patterns in the developing *Xenopus* visual system (Campbell et al., 2001; de la Torre et al., 1997). It is likely that some combination of the two explanations is at work. These same arguments can be used to explain why axon extension was differentially affected at the optic chiasm and in the diencephalon by the same SB-3CT concentration.

What guidance cues could be affected by MMP inhibition? Aside from the optic chiasm, little is known about the guidance pathways involved at each of the decision points within the

diencephalon (Dingwell et al., 2000; Mason and Erskine, 2000; Oster et al., 2004; Williams et al., 2004). Intriguingly, metalloproteinases have been implicated in the processing of either the cue or the receptor of all those that are known. Possible metalloproteinase targets at the optic chiasm are Slits or their receptors, Robos. This signalling system is required for proper axon guidance at the optic chiasm both in mouse and zebrafish (Fricke et al., 2001; Plump et al., 2002). Mice that are double mutant for *slit1* and *slit2* have significant numbers of axons that project into the contralateral optic nerve (Plump et al., 2002), similar to what we observed with metalloproteinase inhibition. Whether MMPs directly cleave either Slits or Robos is unknown. However, *kuzbanian*, the *Drosophila* homologue of ADAM10, interacts genetically with *slit* and *robo* (Schimmelpfeng et al., 2001). It has been proposed that Slits act to channel RGC axons at the optic chiasm (Fricke et al., 2001; Plump et al., 2002). Potentially, preventing normal cleavage of Slits or Robos interferes with this mechanism and results in axons that either aberrantly enter the contralateral optic nerve or defasciculate.

Metalloproteinase-sensitive targets at the optic tectum could include the FGF and netrin guidance pathways. Interestingly, we have found that both inhibiting and promoting FGF signalling produces a RGC axon target recognition defect similar to that observed with the MMP inhibitor (McFarlane et al., 1996; McFarlane et al., 1995). MMP2 can release the soluble ectodomain of FGFR1 (Levi et al., 1996). We observed that GM6001 inhibited FGF2 stimulated RGC neurite extension in vitro (data not shown), which suggests a scenario where an MMP-cleaved FGFR ectodomain would function to promote FGF2 actions on RGC axons. In general, however, soluble FGFR ectodomains are thought to act as inhibitors of FGF signalling (Celli et al., 1998; Guillonneau et al., 1998; Mandler and Neubuser, 2004). Possibly, then, the GM6001/SB-3CT mechanism involves blocked cleavage of heparan sulfate proteoglycans (HSPGs) by growth cone metalloproteinases. Metalloproteinases can cleave HSPGs, and soluble heparan sulfate promotes FGF signalling (Endo et al., 2003; Winkler et al., 2002). As the normal presentation of FGF cues involved in RGC axon target recognition also appears to depend on HSPGs (McFarlane et al., 1996; McFarlane et al., 1995; Walz et al., 1997), interference with HSPG processing either in RGC axons or brain neuroepithelial cells could explain the axon target recognition defects we observed with metalloproteinase inhibition. An alternate explanation involves the netrin 1 receptor, DCC, which is also cleaved by metalloproteinases (Galko and Tessier-Lavigne, 2000). Because in this in vitro study broad-spectrum metalloproteinase inhibitors were used, it was not determined whether an ADAM or MMP was important for cleavage. In *Xenopus*, netrin 1 is expressed deep to the termination field of axons within the optic tectum, and in vitro netrin repulses RGC growth cones at a stage when they innervate the tectum (Shewan et al., 2002). Thus, an inhibitor of DCC cleavage might sensitize RGC axons to netrin and cause them to avoid the tectum altogether, the phenotype we observed with the MMP inhibitor.

Our data argue that an MMP, possibly MMP2, functions in the guidance of RGC axons at several different decision points within the brain. An alternate metalloproteinase, however, functions in the guidance of these axons at the mid-

diencephalon. Future experiments will need to identify the specific metalloproteinases important in guidance of RGC axons at each decision point, and address their potential targets.

References

Agapova, O. A., Ricard, C. S., Salvador-Silva, M. and Hernandez, M. R. (2001). Expression of matrix metalloproteinases and tissue inhibitors of metalloproteinases in human optic nerve head astrocytes. *Glia* **33**, 205-216.

Aye, M. M., Ma, C., Lin, H., Bower, K. A., Wiggins, R. C. and Luo, J. (2004). Ethanol-induced in vitro invasion of breast cancer cells: the contribution of MMP-2 by fibroblasts. *Int. J. Cancer* **112**, 738-746.

Brown, S., Bernardo, M. M., Zhi-Hong, L., Kotra, L. P., Tanaka, Y., Fridman, R. and Mobashery, S. (2000). Potent and selective mechanism-based inhibition of gelatinases. *J. Am. Chem. Soc.* **122**, 6799-6800.

Campbell, D. S., Regan, A. G., Lopez, J. S., Tannahill, D., Harris, W. A. and Holt, C. E. (2001). Semaphorin 3A elicits stage-dependent collapse, turning, and branching in Xenopus retinal growth cones. *J. Neurosci.* **21**, 8538-8547.

Carinato, M. E., Walter, B. E. and Henry, J. J. (2000). Xenopus laevis gelatinase B (Xmmp-9): development, regeneration, and wound healing. *Dev. Dyn.* **217**, 377-387.

Celli, G., LaRochelle, W. J., Mackem, S., Sharp, R. and Merlino, G. (1998). Soluble dominant-negative receptor uncovers essential roles for fibroblast growth factors in multi-organ induction and patterning. *EMBO J.* **17**, 1642-1655.

Chambaut-Guerin, A. M., Herigault, S., Rouet-Benzineb, P., Rouher, C. and Lafuma, C. (2000). Induction of matrix metalloproteinase MMP-9 (92-kDa gelatinase) by retinoic acid in human neuroblastoma SKNBE cells: relevance to neuronal differentiation. *J. Neurochem.* **74**, 508-517.

Chen, J. H., Wu, W., Li, H. S., Fagaly, T., Zhou, L., Wu, J. Y. and Rao, Y. (2000). Embryonic expression and extracellular secretion of Xenopus slit. *Neuroscience* **96**, 231-236.

Chien, C. B., Rosenthal, D. E., Harris, W. A. and Holt, C. E. (1993). Navigational errors made by growth cones without filopodia in the embryonic Xenopus brain. *Neuron* **11**, 237-251.

Cornel, E. and Holt, C. (1992). Precocious pathfinding: retinal axons can navigate in an axonless brain. *Neuron* **9**, 1001-1011.

Damjanovski, S., Puzianowska-Kuznicka, M., Ishuzuya-Oka, A. and Shi, Y. B. (2000). Differential regulation of three thyroid hormone-responsive matrix metalloproteinase genes implicates distinct functions during frog embryogenesis. *FASEB J.* **14**, 503-510.

de la Torre, J. R., Hopker, V. H., Ming, G. L., Poo, M. M., Tessier-Lavigne, M., Hemmati-Brivanlou, A. and Holt, C. E. (1997). Turning of retinal growth cones in a netrin-1 gradient mediated by the netrin receptor DCC. *Neuron* **19**, 1211-1224.

Diaz-Rodriguez, E., Cabrera, N., Esparis-Ogando, A., Montero, J. C. and Pandiella, A. (1999). Cleavage of the TrkA neurotrophin receptor by multiple metalloproteases generates signalling-competent truncated forms. *Eur. J. Neurosci.* **11**, 1421-1430.

Dingwell, K. S., Holt, C. E. and Harris, W. A. (2000). The multiple decisions made by growth cones of RGCs as they navigate from the retina to the tectum in Xenopus embryos. *J. Neurobiol.* **44**, 246-259.

Endo, K., Takino, T., Miyamori, H., Kinsen, H., Yoshizaki, T., Furukawa, M. and Sato, H. (2003). Cleavage of syndecan-1 by membrane type matrix metalloproteinase-1 stimulates cell migration. *J. Biol. Chem.* **278**, 40764-40770.

Fambrough, D., Pan, D., Rubin, G. M. and Goodman, C. S. (1996). The cell surface metalloprotease/disintegrin Kuzbanian is required for axonal extension in Drosophila. *Proc. Natl. Acad. Sci. USA* **93**, 13233-13238.

Fricke, C., Lee, J. S., Geiger-Rudolph, S., Bonhoeffer, F. and Chien, C. B.

(2001). astray, a zebrafish roundabout homolog required for retinal axon guidance. *Science* **292**, 507-510.

Galko, M. J. and Tessier-Lavigne, M. (2000). Function of an axonal chemoattractant modulated by metalloprotease activity. *Science* **289**, 1365-1367.

Guillonneau, X., Regnier-Ricard, F., Laplace, O., Jonet, L., Bryckaert, M., Courtois, Y. and Mascarelli, F. (1998). Fibroblast growth factor (FGF) soluble receptor 1 acts as a natural inhibitor of FGF2 neurotrophic activity during retinal degeneration. *Mol. Biol. Cell* **9**, 2785-2802.

Hattori, M., Osterfield, M. and Flanagan, J. G. (2000). Regulated cleavage of a contact-mediated axon repellent. *Science* **289**, 1360-1365.

Hayashita-Kinoh, H., Kinoh, H., Okada, A., Komori, K., Itoh, Y., Chiba, T., Kajita, M., Yana, I. and Seiki, M. (2001). Membrane-type 5 matrix metalloproteinase is expressed in differentiated neurons and regulates axonal growth. *Cell Growth Differ.* **12**, 573-580.

Holt, C. E. (1989). A single-cell analysis of early retinal ganglion cell differentiation in Xenopus: from soma to axon tip. *J. Neurosci.* **9**, 3123-3145.

Huang, X., Huang, P., Robinson, M. K., Stern, M. J. and Jin, Y. (2003). UNC-71, a disintegrin and metalloprotease (ADAM) protein, regulates motor axon guidance and sex myoblast migration in C. elegans. *Development* **130**, 3147-3161.

Isaksen, B. and Fagerhol, M. K. (2001). Calprotectin inhibits matrix metalloproteinases by sequestration of zinc. *Mol. Pathol.* **54**, 289-292.

Johnson, L. L., Dyer, R. and Hupe, D. J. (1998). Matrix metalloproteinases. *Curr. Opin. Chem. Biol.* **2**, 466-471.

Jung, J. C., Leco, K. J., Edwards, D. R. and Fini, M. E. (2002). Matrix metalloproteinases mediate the dismantling of mesenchymal structures in the tadpole tail during thyroid hormone-induced tail resorption. *Dev. Dyn.* **223**, 402-413.

Kleifeld, O., Kotra, L. P., Gervasi, D. C., Brown, S., Bernardo, M. M., Fridman, R., Mobashery, S. and Sagi, I. (2001). X-ray absorption studies of human matrix metalloproteinase-2 (MMP-2) bound to a highly selective mechanism-based inhibitor. Comparison with the latent and active forms of the enzyme. *J. Biol. Chem.* **276**, 17125-17131.

Koivunen, E., Arap, W., Valtanen, H., Rainisalo, A., Medina, O. P., Heikkila, P., Kantor, C., Gahmberg, C. G., Salo, T., Konttinen, Y. T. et al. (1999). Tumor targeting with a selective gelatinase inhibitor. *Nat. Biotechnol.* **17**, 768-774.

Leighton, P. A., Mitchell, K. J., Goodrich, L. V., Lu, X., Pinson, K., Scherz, P., Skarnes, W. C. and Tessier-Lavigne, M. (2001). Defining brain wiring patterns and mechanisms through gene trapping in mice. *Nature* **410**, 174-179.

Levi, E., Fridman, R., Miao, H. Q., Ma, Y. S., Yayon, A. and Vlodavsky, I. (1996). Matrix metalloproteinase 2 releases active soluble ectodomain of fibroblast growth receptor 1. *Proc. Natl. Acad. Sci. USA* **93**, 7069-7074.

Mandler, M. and Neubuser, A. (2004). FGF signaling is required for initiation of feather placode development. *Development* **131**, 3333-3343.

Mason, C. and Erskine, L. (2000). Growth cone form, behavior, and interactions in vivo: retinal axon pathfinding as a model. *J. Neurobiol.* **44**, 260-270.

McFarlane, S. (2003). Metalloproteases: carving out a role in axon guidance. *Neuron* **37**, 559-562.

McFarlane, S. (2005). Metalloproteinases in development: breaking things down to build a nervous system. In *MMPs and the Nervous System* (ed. K. Conant and P. Gottschall), pp. 153-187. London: Imperial College Press.

McFarlane, S., McNeill, L. and Holt, C. E. (1995). FGF signaling and target recognition in the developing Xenopus visual system. *Neuron* **15**, 1017-1028.

McFarlane, S., Cornel, E., Amaya, E. and Holt, C. E. (1996). Inhibition of FGF receptor activity in retinal ganglion cell axons causes errors in target recognition. *Neuron* **17**, 245-254.

Mechtersheimer, S., Gutwein, P., Agmon-Levin, N., Stoeck, A., Oleszewski, M., Riedle, S., Postina, R., Fahrenholz, F., Fogel, M., Lemmon, V. et al. (2001). Ectodomain shedding of L1 adhesion molecule promotes cell migration by autocrine binding to integrins. *J. Cell Biol.* **155**, 661-673.

Naus, S., Richter, M., Wildeboer, D., Moss, M., Schachner, M. and Bartsch, J. W. (2004). Ectodomain shedding of the neural recognition molecule CHL1 by the metalloprotease-disintegrin ADAM8 promotes neurite outgrowth and suppresses neuronal cell death. *J. Biol. Chem.* **279**, 16083-16090.

Nieuwkoop, P. D. and Faber, J. (1994). *Normal table of* Xenopus laevis *(Daudin).* New York, NY: Garland.

Nishiwaki, K., Hisamoto, N. and Matsumoto, K. (2000). A metalloprotease disintegrin that controls cell migration in Caenorhabditis elegans. *Science* **288**, 2205-2208.

Nordstrom, L. A., Lochner, J., Yeung, W. and Ciment, G. (1995). The metalloproteinase stromelysin-1 (transin) mediates PC12 cell growth cone invasiveness through basal laminae. *Mol. Cell. Neurosci.* **6**, 56-68.

Oster, S. F., Deiner, M., Birgbauer, E. and Sretavan, D. W. (2004). Ganglion cell axon pathfinding in the retina and optic nerve. *Semin. Cell Dev. Biol.* **15**, 125-136.

Page-McCaw, A., Serano, J., Sante, J. M. and Rubin, G. M. (2003). Drosophila matrix metalloproteinases are required for tissue remodeling, but not embryonic development. *Dev. Cell* **4**, 95-106.

Plump, A. S., Erskine, L., Sabatier, C., Brose, K., Epstein, C. J., Goodman, C. S., Mason, C. A. and Tessier-Lavigne, M. (2002). Slit1 and Slit2 cooperate to prevent premature midline crossing of retinal axons in the mouse visual system. *Neuron* **33**, 219-232.

Prada, F. A., Dorado, M. E., Quesada, A., Prada, C., Schwarz, U. and de la Rosa, E. J. (1995). Early expression of a novel radial glia antigen in the chick embryo. *Glia* **15**, 389-400.

Schimmelpfeng, K., Gogel, S. and Klambt, C. (2001). The function of leak and kuzbanian during growth cone and cell migration. *Mech. Dev.* **106**, 25-36.

Shewan, D., Dwivedy, A., Anderson, R. and Holt, C. E. (2002). Age-related changes underlie switch in netrin-1 responsiveness as growth cones advance along visual pathway. *Nat. Neurosci.* **5**, 955-962.

Sive, H. L., Grainger, R. M. and Harland, R. M. (2000). *Early Development of* Xenopus laevis*: A Laboratory Manual.* Cold Spring Harbor: Cold Spring Harbor Laboratory Press.

Walz, A., McFarlane, S., Brickman, Y. G., Nurcombe, V., Bartlett, P. F. and Holt, C. E. (1997). Essential role of heparan sulfates in axon navigation and targeting in the developing visual system. *Development* **124**, 2421-2430.

Webber, C. A., Hocking, J. C., Yong, V. W., Stange, C. L. and McFarlane, S. (2002). Metalloproteases and guidance of retinal axons in the developing visual system. *J. Neurosci.* **22**, 8091-8100.

Webber, C. A., Hyakutake, M. T. and McFarlane, S. (2003). Fibroblast growth factors redirect retinal axons in vitro and in vivo. *Dev. Biol.* **263**, 24-34.

Williams, S. E., Mason, C. A. and Herrera, E. (2004). The optic chiasm as a midline choice point. *Curr. Opin. Neurobiol.* **14**, 51-60.

Winkler, S., Stahl, R. C., Carey, D. J. and Bansal, R. (2002). Syndecan-3 and perlecan are differentially expressed by progenitors and mature oligodendrocytes and accumulate in the extracellular matrix. *J. Neurosci. Res.* **69**, 477-487.

Yong, V. W., Power, C., Forsyth, P. and Edwards, D. R. (2001). Metalloproteinases in biology and pathology of the nervous system. *Nat. Rev. Neurosci.* **2**, 502-511.

Zuo, J., Ferguson, T. A., Hernandez, Y. J., Stetler-Stevenson, W. G. and Muir, D. (1998). Neuronal matrix metalloproteinase-2 degrades and inactivates a neurite-inhibiting chondroitin sulfate proteoglycan. *J. Neurosci.* **18**, 5203-5211.